UDC 621.3 https://doi.org/10.20998/2074-272X.2025.6.02

T. Bessaad, A. Benbouali, K. Khelifi Otmane, R. Taleb, H. Sahraoui, A. Iqbal

Inverter fuzzy speed control of multi-machine system series-connected fed by a single five-phase an asymmetrical 19-level inverter with less number of switches

Introduction. *5-phase permanent magnet synchronous machines (PMSMs) are widely used in modern electric drive systems due to their superior torque density, improved fault tolerance, and reduced torque ripple. These characteristics make them ideal for demanding applications such as electric vehicles, aerospace systems, and industrial automation.* ***Problem***. *Despite their advantages, conventional multi-machine systems using multilevel inverters and PI controllers suffer from sensitivity to parameter variations, high torque ripple, and increased cost and complexity due to the large number of power switches. The* ***goal*** *of this work is to design and validate a compact robust drive system that enables independent vector control of two series-connected 5-phase PMSMs using a reduced switch count asymmetrical 19-level inverter and fuzzy logic controllers.* ***Methodology***. *The proposed system is modeled in the phase domain and transformed using Clarke and Park transformations to enable decoupled control. Mamdani-type fuzzy logic controllers are implemented for both speed and current regulation. The system is simulated in MATLAB/Simulink to evaluate performance under dynamic conditions and parameter variations.* ***Results***. *The fuzzy logic controller significantly outperforms the conventional PI controller, achieving a settling time of 0.06 s versus 0.15 s, a steady-state speed error of 0.4 % compared to 1.9 %, and a torque ripple reduction of 47 %. Under robustness testing with doubled inertia, the fuzzy controller maintains stable and accurate control, whereas the PI controller fails. Additionally, the inverter achieves near-sinusoidal output with a total harmonic distortion of less than 4.5 %, and the switch count is reduced by 66 % compared to traditional 36-switch designs.* ***Scientific novelty***. *This work presents the first implementation of independent vector control for two series-connected PMSMs using a single 12-switch asymmetrical 19-level inverter and model-free fuzzy logic control, offering a simpler and more efficient alternative to existing approaches.* ***Practical value***. *The proposed system provides a highly efficient and cost-effective solution for electric drive applications where space, reliability, and control robustness are essential, such as in electric transportation, avionics, and compact industrial systems.* References 26, tables 4, figures 9.

Key words: **multi-machine system, fuzzy logic controller, independent vector control, asymmetric inverter.**

Вступ. *П'ятифазні синхронні машини з постійними магнітами (PMSMs) широко використовуються в сучасних системах електроприводу завдяки високій щільності і зменшеній пульсації крутного моменту, та підвищеній відмовостійкості. Ці характеристики роблять їх ідеальними для багатьох застосувань – електромобілі, аерокосмічні системи та промислова автоматика.* ***Проблема***. *Незважаючи на переваги, традиційні багатомашинні системи, що використовують багаторівневі інвертори та ПІ-регулятори, є чутливими до змін параметрів, високої пульсації крутного моменту, а також високій вартості і складності через велику кількість силових ключів.* ***Метою*** *роботи є розробка та валідація компактної надійної системи приводу, яка забезпечує незалежне векторне керування двома послідовно з'єднаними п'ятифазними PMSM з використанням асиметричного 19-рівневого інвертора зі зменшеною кількістю ключів та нечітких логічних контролерів.* ***Методологія***. *Запропонована система моделюється у фазовій області з використанням перетворень Кларка та Парка для забезпечення розв'язаного керування. Реалізовано нечіткі логічні контролери типу Мамдані для регулювання швидкості і струму. Система моделюється в MATLAB/Simulink для оцінки продуктивності в динамічних умовах та зміни параметрів.* ***Результати***. *Нечіткий логічний регулятор значно перевершує традиційний ПІ-регулятор, досягаючи часу встановлення 0,06 с проти 0,15 с, помилки швидкості 0,4 % проти 1,9 % і зниження пульсацій крутного моменту на 47 %. При випробуванні на надійність з подвоєним моментом інерції нечіткий логічний регулятор підтримує стабільне та точне керування, тоді як ПІ-регулятор виходить з ладу. Крім того, інвертор досягає майже синусоїдального вихідного сигналу із загальним коефіцієнтом гармонічних спотворень менше 4,5 %, а кількість перемикачів скорочено на 66 % порівняно з традиційними конструкціями з 36 перемикачами.* ***Наукова новизна***. *У роботі представлена перша реалізація незалежного векторного управління для двох послідовно з'єднаних PMSMs з використанням одного асиметричного 19-рівневого інвертора з 12 перемикачами та нечіткого логічного управління без моделі, що пропонує більш просту та ефективну альтернативу існуючим підходам.* ***Практична значимість***. *Пропонована система є високоефективним та економічним рішенням для електроприводів, де важливі компактність, надійність і стійкість управління, наприклад, в електротранспорті, авіоніці та компактних промислових системах.* Бібл. 26, табл. 4, рис. 9.

Ключові слова: **багатомашинна система, контролер нечіткої логіки, незалежне векторне керування, асиметричний інвертор.**

Introduction. Multi-phase machines have attracted growing interest due to their numerous advantages over conventional 3-phase systems. These include reduced current ripple [1], improved stability and fault tolerance [2], higher torque density [3, 4], and lower torque pulsations [5, 6]. Such characteristics make them well-suited for demanding applications such as electric aircraft, marine propulsion, robotics, and hybrid/electric vehicles [7, 8]. Among the various configurations, dual-machine drive systems, where two multi-phase machines are connected in series or parallel and powered by voltage- and frequency-controlled sources, typically multilevel inverters (MLIs), have proven particularly promising [9, 10]. These systems support independent motor operation under different load and speed conditions, enabling flexible control strategies and the use of various motor types [11].

Effective control of such systems requires managing additional stator current components beyond those needed for single-machine vector control. When the stator windings are connected in series, each machine can effectively operate as though it were supplied by an independent multi-phase voltage source [12], as demonstrated in 5-phase systems powered by a single inverter [13, 14]. To meet high-voltage demands in electric traction applications, MLIs have emerged as the preferred solution [14], with typical topologies including neutral point clamped inverters [15], flying capacitor inverters [16], and cascaded H-bridge inverters [17]. While cascaded H-bridge architectures offer benefits such as modularity and reduced voltage stress [18], increasing the number of output levels usually requires more switching devices, which adds to system complexity and cost [19].

Recent advances have introduced 19-level asymmetrical inverter architectures that use significantly fewer switches, such as 9-switch or 12-switch designs, without compromising output quality [20]. The present study proposes a compact 19-level asymmetrical 5-phase inverter architecture that drives two series-connected 5-phase permanent magnet synchronous machines (PMSMs) using only 12 switches, while maintaining high-quality voltage output [21]. To control the system, we employ fuzzy logic control (FLC) for both speed and current regulation. Unlike traditional methods, FLC does not require an accurate mathematical model and is inherently robust to parameter variations. Comparative results demonstrate that the proposed FLC significantly outperforms conventional PI control under dynamic load conditions, while also reducing total harmonic distortion (THD).

The **goal** of this work is to design and validate a compact robust drive system that enables independent vector control of two series-connected 5-phase PMSMs using a reduced-switch-count asymmetrical 19-level inverter and fuzzy logic controllers.

Asymmetrical MLI with uniform step configuration. A detailed schematic of the partial cells is shown in Fig. 1, which also shows the main notation conventions adopted throughout this study. The switching states of the transistor pairs S_{jx}/S'_{jx} (for x=1,2 and j=1 to k) are controlled by binary signals M_{jx} and M'_{jx}, respectively. These Boolean control functions are subject to the following logical constraints:

$$M_{jx} + M'_{jx} = 1 . \quad (1)$$

A dedicated conversion function F_j maps the switching states to their corresponding voltage levels:

$$F_j = M_{jx} - M'_{jx} \Rightarrow F_j \in \{-1, 0, +1\}. \quad (2)$$

The output voltage generated by each power cell is defined as:

$$U_{pj} = F_j \cdot U_{dj} \Rightarrow U_{pj} \in \{-U_{dj}, 0, +U_{dj}\}, \quad (3)$$

which illustrates the ternary voltage-level generation capability of each individual partial cell. When combined, the total output voltage of the complete MLI is:

$$U_s = U_{p1} + U_{p2} + \cdots U_{pk} , \quad (4)$$

where $U_{p1} - U_p$ are the output voltages from each partial inverter cell (or module); U_s is the total synthesized output voltage at the inverter terminal.

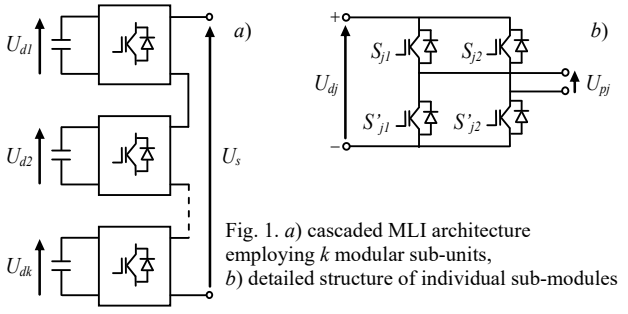

Fig. 1. *a*) cascaded MLI architecture employing k modular sub-units, *b*) detailed structure of individual sub-modules

The asymmetric configuration of MLIs is defined by the use of non-uniform DC input voltages, where at least one partial inverter is supplied with a different voltage level from its series-connected counterparts. In regular-step asymmetric MLI topologies, 3 design criteria must be satisfied to achieve equal voltage steps (ΔU) across all output levels. Importantly, this uniform step size is directly determined by the smallest DC voltage source in the system, denoted as U_{d1} [22].

Successful operation of the asymmetrical MLI depends on satisfying the following design conditions:

1) monotonic ordering of DC inputs. The DC voltage sources must be arranged in a strictly monotonically increasing sequence, such that: $U_{d(h-1)} \le U_{dh}$, $\forall\ h = 2 \ldots k$;

2) voltage ratio constraint. The ratio between 2 consecutive DC sources must satisfy: $U_{dh}/U_{d(h-1)} = \delta_h$, $\delta_h \in N^*$;

3) dedicated DC source per cell. Each j^{th} cell in the cascaded structure must be supplied with a distinct DC voltage U_{dj}, such that:

$$U_{dj} \le 1 + 2\sum_{l=1}^{j-1} U_{dl} . \quad (5)$$

If all these conditions are fulfilled, the inverter can generate an output voltage waveform U_s consisting of N equally spaced voltage levels:

$$N = 1 + 2\sum_{j=1}^{k} \left(U_{dj} / U_{d1}\right). \quad (6)$$

For k=3 in (6), the 13-level output voltage waveform can be synthesized using 2 distinct sets of DC source configurations, i.e., (U_{d1}, U_{d2}, U_{d3})∈{(1, 1, 4), (1, 2, 3)}. Figure 2 shows the complete set of output voltage combinations achievable by the 3 partial cells (k=3) in the 9-level inverter topology. The corresponding DC voltage values for the 3 cells are: U_{d1} = 1 p.u., U_{d2} = 1 p.u., U_{d3} = 2 p.u. Each partial inverter generates one of 3 possible output voltage levels: U_{p1}∈{–1, 0, 1}, U_{p2}∈{–1, 0, 1} and U_{p3}∈{–2, 0, 2}. This configuration enables the proposed topology to synthesize a 9-level output voltage waveform: U_s∈{–4, –3, –2, –1, 0, 1, 2, 3, 4}. Certain output voltage values can be obtained using multiple switching combinations. For example, the 2 p.u. output voltage can be achieved through the following 4 distinct switching states: (U_{p1}, U_{p2}, U_{p3})∈{(–1, 1, 2), (0, 0, 2), (1, –1, 2), (1, 1, 0)}. The existence of multiple voltage synthesis paths, including redundant switching states for the same output level, introduces degrees of freedom that can be strategically exploited. These degrees of freedom enhance the performance of the uniform step asymmetrical MLI in terms of efficiency, reliability, and power quality [23].

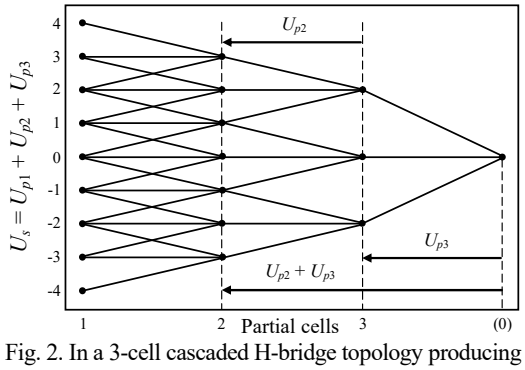

Fig. 2. In a 3-cell cascaded H-bridge topology producing 9 voltage levels, the possible output states per partial inverter are: (U_{d1} = 1 p.u.; U_{d2} = 1 p.u.; U_{d3} = 2 p.u.)

Asymmetrical MLIs offer the user a high degree of design flexibility, particularly through the ability to select different intermediate voltage levels and the availability of redundancy in these choices.

The approach utilizes two fundamental control variables [21, 24]: Modulation index m and modulation rate r:

$$m = f_c / f_r \ ; \tag{7}$$

$$r = 2A_r / (N-1)A_c \ . \tag{8}$$

Table 1 shows representative DC voltage configurations along with their corresponding output voltage level capabilities. The case study focuses on a 3-stage (k=3) series-connected single-phase inverter topology for each phase leg.

Table 1

Voltage imbalance phenomena in 3-cell uniform step asymmetrical MLI systems

N	u_{d1}, p.u	u_{d2}, p.u	u_{d3}, p.u
7	1	1	1
9	1	1	2
11	1	1	3
	1	2	2
13	1	1	4
	1	2	3
15	1	1	5
	1	2	4
	1	3	3
17	1	1	6
	1	2	5
	1	3	4
19	1	1	7
	1	2	6
	1	3	5
	1	4	4

The multi-machine system (Fig. 3) consists of two 5-phase PMSMs connected in series. A single 5-phase inverter supplies power to both machines. Each machine exhibits a spatial phase shift of 72° between 2 successive stator phases.

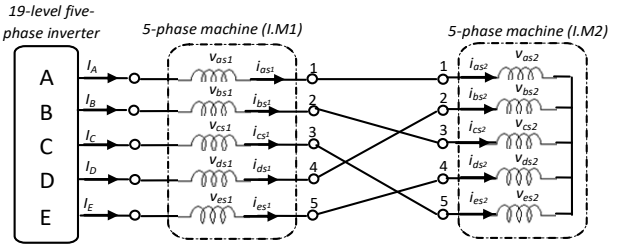

Fig. 3. Diagram of coupling the phase windings in series of the stator of the multi-motors (a 5-phase inverter powers the system)

In the analysis, it is assumed that both machines have identical electrical parameters. The electrical circuit of the system is described as:

$$[\boldsymbol{V}_{\boldsymbol{ABCDE}}] = [R_S][\boldsymbol{i}_{\boldsymbol{ABCDE}}] + \frac{\mathrm{d}}{\mathrm{d}t}[\varphi_{\boldsymbol{ABCDE}}], \tag{9}$$

where V_{ABCDE} is the vector of stator voltages each phase (A to E); i_{ABCDE} is the vector of phase currents; R_s *is* the stator resistance (assumed equal for all phases); φ_{ABCDE} is the vector of stator flux linkages.

Figure 3 illustrates the relationship between the stator winding voltages and the source currents for two 5-phase PMSMs connected in series. The stator winding phases (A–E) and the neutral point (N) correspond to the inverter's output terminals.

The stator voltages of the 2 machines are given by:

$$[\boldsymbol{V_s}] = \begin{bmatrix} v_A \\ v_B \\ v_C \\ v_D \\ v_E \end{bmatrix} = \begin{bmatrix} v_{as1} + v_{as2} \\ v_{bs1} + v_{cs2} \\ v_{cs1} + v_{es2} \\ v_{ds1} + v_{bs2} \\ v_{es1} + v_{ds2} \end{bmatrix}, \tag{10}$$

where $v_{as1,2}$, $v_{bs1,2}$, $v_{cs1,2}$, $v_{ds1,2}$, $v_{es1,2}$ are the phase voltages of 2 machines.

The following equation represents the stator currents of the two 5-phase machines connected in series. Phases A–E and the neutral point N correspond to the MLI's output. Figure 3 also shows the connection between each machine's source and stator currents:

$$[\boldsymbol{i_s}] = \begin{bmatrix} i_A \\ i_B \\ i_C \\ i_D \\ i_E \end{bmatrix} = \begin{bmatrix} i_{as1} \\ i_{bs1} \\ i_{cs1} \\ i_{ds1} \\ i_{es1} \end{bmatrix} = \begin{bmatrix} i_{as2} \\ i_{cs2} \\ i_{es2} \\ i_{bs2} \\ i_{ds2} \end{bmatrix}, \tag{11}$$

where $i_{as1,2}$, $i_{bs1,2}$, $i_{cs1,2}$, $i_{ds1,2}$, $i_{es1,2}$ are the currents of 2 machines.

The power-invariant Clarke decoupling transformation matrix is:

$$[C]^t = \sqrt{\frac{2}{5}} \begin{bmatrix} 1 & \cos(\alpha) & \cos(2\alpha) & \cos(3\alpha) & \cos(4\alpha) \\ 0 & \sin(\alpha) & \sin(2\alpha) & \sin(3\alpha) & \sin(4\alpha) \\ 1 & \cos(2\alpha) & \cos(4\alpha) & \cos(6\alpha) & \cos(8\alpha) \\ 0 & \sin(2\alpha) & \sin(4\alpha) & \sin(6\alpha) & \sin(8\alpha) \\ 1/\sqrt{2} & 1/\sqrt{2} & 1/\sqrt{2} & 1/\sqrt{2} & 1/\sqrt{2} \end{bmatrix}. \tag{12}$$

Moving to the new variables system (α,β,x,y,o) from the original system (A–E), we have:

$$f(\alpha\beta xy) = [\boldsymbol{C}] \cdot f(\mathrm{ABCDE}),$$

where $[\boldsymbol{C}]$ is the power-invariant transformation matrix.

The voltages and currents of the 5-phase inverter (α, β) and (x, y) axes are defined as:

$$\begin{bmatrix} v_\alpha^{inv} \\ v_\beta^{inv} \\ v_x^{inv} \\ v_y^{inv} \\ v_o^{inv} \end{bmatrix} = [\boldsymbol{C}] \begin{bmatrix} v_A \\ v_B \\ v_C \\ v_D \\ v_E \end{bmatrix} = [\boldsymbol{C}] \begin{bmatrix} v_{as1} + v_{as2} \\ v_{bs1} + v_{cs2} \\ v_{cs1} + v_{es2} \\ v_{ds1} + v_{bs2} \\ v_{es1} + v_{ds2} \end{bmatrix} = [\boldsymbol{C}] \begin{bmatrix} v_{\alpha s1} + v_{xs2} \\ v_{\beta s1} + v_{ys2} \\ v_{xs1} + v_{\alpha s2} \\ v_{ys1} + v_{\beta s2} \\ 0 \end{bmatrix}; \tag{13}$$

$$\begin{cases} i_\alpha^{inv} = i_{\alpha s1} = i_{xs2}; \\ i_\beta^{inv} = i_{\beta s1} = -i_{ys2}; \\ i_x^{inv} = i_{xs1} = i_{\alpha s2}; \\ i_y^{inv} = i_{ys1} = i_{\beta s2}, \end{cases} \tag{14}$$

where v_α^{inv}, v_β^{inv}, v_x^{inv}, v_y^{inv} and i_α^{inv}, i_β^{inv}, i_x^{inv}, i_y^{inv} are the inverter voltage and currents in the $\alpha\beta$ and xy axes.

Since the two subspaces $\alpha\beta$ and xy are orthogonal (Fig. 3) the chosen series connection strategy enables independent vector control of the two machines.

The zero-sequence component of the MLI can be neglected. The electromagnetic part of the drive system is described by 8 first-order equations. Equations (15), (16) represent the 4 inverter/stator voltage expressions:

$$\begin{cases} v_\alpha^{inv} = (R_{s1}+R_{s2})i_\alpha^{inv} + (L_{sl1}+\frac{5}{2}M_{s1})\frac{\mathrm{d}}{\mathrm{d}t}i_\alpha^{inv} + \\ \quad + L_{sl2}\frac{\mathrm{d}}{\mathrm{d}t}i_\alpha^{inv} - \sqrt{\frac{5}{2}}\Omega_1\phi_{f1}\sin\theta_1; \\ v_\beta^{inv} = (R_{s1}+R_{s2})i_\beta^{inv} + (L_{sl1}+\frac{5}{2}M_{s1})\frac{\mathrm{d}}{\mathrm{d}t}i_\beta^{inv} + \\ \quad + L_{sl2}\frac{\mathrm{d}}{\mathrm{d}t}i_\beta^{inv} + \sqrt{\frac{5}{2}}\Omega_1\phi_{f1}\cos\theta_1; \end{cases} \quad (15)$$

$$\begin{cases} v_x^{inv} = (R_{s1}+R_{s2})i_x^{inv} + (L_{sl2}+\frac{5}{2}M_{s2})\frac{\mathrm{d}}{\mathrm{d}t}i_x^{inv} + \\ \quad + L_{sl1}\frac{\mathrm{d}}{\mathrm{d}t}i_x^{inv} - \sqrt{\frac{5}{2}}\Omega_2\phi_{f2}\sin\theta_2; \\ v_y^{inv} = (R_{s1}+R_{s2})i_y^{inv} + (L_{sl2}+\frac{5}{2}M_{s2})\frac{\mathrm{d}}{\mathrm{d}t}i_y^{inv} + \\ \quad + L_{sl1}\frac{\mathrm{d}}{\mathrm{d}t}i_y^{inv} + \sqrt{\frac{5}{2}}\Omega_2\phi_{f2}\cos\theta_2, \end{cases} \quad (16)$$

where $L_{sl1,2}$, $M_{s1,2}$ are the inductance and mutual inductance in the rotating frame; $\Omega_{1,2}$, $\phi_{f1,2}$, $\theta_{1,2}$ are the mechanical speed, flux and electrical speed, respectively.

To achieve a more compact representation, the stator parameters are transformed into a φ-rotated (dq) synchronous reference frame from the stationary ($\alpha\beta$) frame using the transformation matrix [$\boldsymbol{D}$]:

$$[\boldsymbol{D}] = \begin{bmatrix} \cos\theta & \sin\theta & . \\ \sin\theta & \cos\theta & . \\ . & . & [I]^{3\times3} \end{bmatrix}. \quad (17)$$

The torque equations for the 2 series-connected machines are:

$$\begin{cases} T_{em1} = p_1[(L_d - L_q)i_d^{inv}\cdot i_q^{inv} + \sqrt{\frac{5}{2}\phi_{f1}}\cdot i_q^{inv}]; \\ T_{em2} = p_2[(L_x - L_y)i_x^{inv}\cdot i_y^{inv} + \sqrt{\frac{5}{2}\phi_{f2}}\cdot i_y^{inv}], \end{cases} \quad (18)$$

where p_1, p_2 are the number of pole pairs for 2 machines.

From the previous equations it is clear that the torque-producing current components i_{sd}, i_{sq} in the 1st machine are set to 0. As a result, the torque is generated by the 2nd machine through the current components i_{sx}, i_{sy}. This configuration allows both machines to be independently controlled using a single voltage source inverter.

Interconnected 5-phase PMSM set in series configuration with independent control loops. The torque control strategy derived in (18) relies on the i_{sd}, i_{sq} currents for the 1st machine, and a similar current-controlled method is applied to the 2nd machine using i_{sx}, i_{sy}. A common strategy in such systems is to set i_{sd} and i_{sx} to 0, ensuring that torque is controlled exclusively by i_{sq} and i_{sy}.

For the 1st machine:

$$\begin{cases} v_d^{inv} = (R_{s1}+R_{s2})i_d^{inv} + (L_{sl1}+\frac{5}{2}M_{s1})\frac{\mathrm{d}}{\mathrm{d}t}i_d^{inv} + \\ \quad + L_{sl2}\frac{\mathrm{d}}{\mathrm{d}t}i_d^{inv} - \Omega_1(L_{sl1}+\frac{5}{2}M_{s1})i_q^{inv}; \\ v_q^{inv} = (R_{s1}+R_{s2})i_q^{inv} + (L_{sl1}+\frac{5}{2}M_{s1})\frac{\mathrm{d}}{\mathrm{d}t}i_q^{inv} + \\ \quad + L_{sl2}\frac{\mathrm{d}}{\mathrm{d}t}i_q^{inv} - \Omega_1(L_{sl1}+\frac{5}{2}M_{s1})i_d^{inv} + \sqrt{\frac{5}{2}}\Omega_1\phi_{f1}. \end{cases} \quad (19)$$

For the 2nd machine:

$$\begin{cases} v_x^{inv} = (R_{s1}+R_{s2})i_x^{inv} + (L_{sl1}+\frac{5}{2}M_{s2})\frac{\mathrm{d}}{\mathrm{d}t}i_x^{inv} + \\ \quad + L_{sl1}\frac{\mathrm{d}}{\mathrm{d}t}i_x^{inv} - \Omega_2(L_{sl2}+\frac{5}{2}M_{s2})i_y^{inv}; \\ v_y^{inv} = (R_{s1}+R_{s2})i_y^{inv} + (L_{sl1}+\frac{5}{2}M_{s2})\frac{\mathrm{d}}{\mathrm{d}t}i_y^{inv} + \\ \quad + L_{sl1}\frac{\mathrm{d}}{\mathrm{d}t}i_y^{inv} - \Omega_2(L_{sl2}+\frac{5}{2}M_{s2})i_x^{inv} + \sqrt{\frac{5}{2}}\Omega_2\phi_{f2}. \end{cases} \quad (20)$$

The overall voltage references are generated based on the schematic shown in Fig. 4, and are defined as [11]:

$$\begin{bmatrix} V_a^* \\ V_b^* \\ V_c^* \\ V_d^* \\ V_e^* \end{bmatrix} = \begin{bmatrix} v_{as1}^* + v_{as2}^* \\ v_{bs1}^* + v_{cs2}^* \\ v_{cs1}^* + v_{es2}^* \\ v_{ds1}^* + v_{bs2}^* \\ v_{es1}^* + v_{ds2}^* \end{bmatrix}, \quad (21)$$

where symbol «*» indicates a reference value provided to the controller.

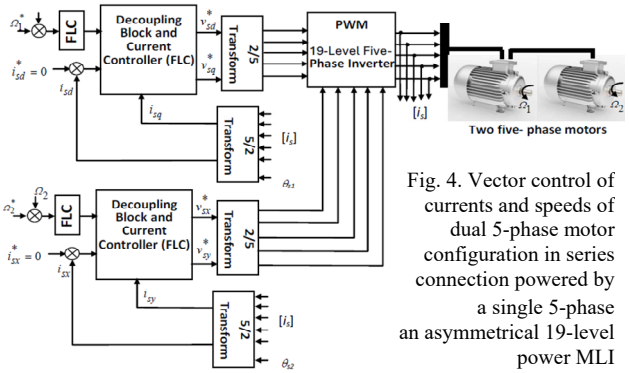

Fig. 4. Vector control of currents and speeds of dual 5-phase motor configuration in series connection powered by a single 5-phase an asymmetrical 19-level power MLI

Machines parameters are listed in Table 2.

Table 2

Machines parameters

R_s, Ω	L_d=L_q, H	J_k, kg/m^2	p	ϕ_f, Wb	f, Hz	F_r, kg·m^2·s^{-1}
3.6	0.0021	0.0011	2	0.25	50	0.0014

Fuzzy logic controller (FLC). FLCs are widely used in the speed control of electric machines due to their simplicity, intuitive design, and model-free nature. Unlike conventional control techniques, FLCs do not require an accurate mathematical model of the system or a complex feedback loop to achieve effective performance.

In an FLC, the input and output variables are defined using membership functions within a common universe of discourse. The controller's performance depends heavily on the appropriate selection of scaling factors (gains) and the careful tuning of its parameters. These settings are often optimized empirically through trial-and-error methods to enhance control quality [25, 26].

A fuzzy logic controller typically consists of 4 main components: a rule base, an inference engine, a fuzzification module, and a defuzzification module. In this study, Mamdani's inference method is applied using the max–min composition technique. To convert fuzzy outputs into crisp control actions, the center of area method is used for defuzzification.

The architecture of the proposed fuzzy speed controller is shown in Fig. 5. It processes 2 input variables – the speed error E and its derivative ΔE. Based

on these inputs, the controller generates an output signal representing the torque increment ΔT_{em}. Integration of this signal provides the electromagnetic torque command T_{em}.

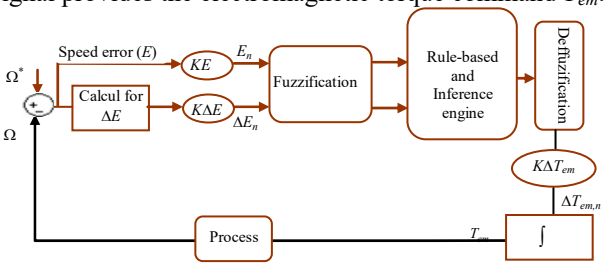

Fig. 5. Block diagram of the fuzzy speed controller

The fuzzy speed controller employs a complete rule base of 49 If–Then rules, covering all possible combinations of input conditions. As shown in Fig. 6, all variables – namely, the speed error E, its time derivative (ΔE), and the output signal – use triangular membership functions. Each variable is divided into 7 linguistic categories: Negative High (NH); Negative Moderate (NM); Negative Low (NS); Neutral (ZE); Positive Low (PS); Positive Moderate (PM); Positive High (PH).

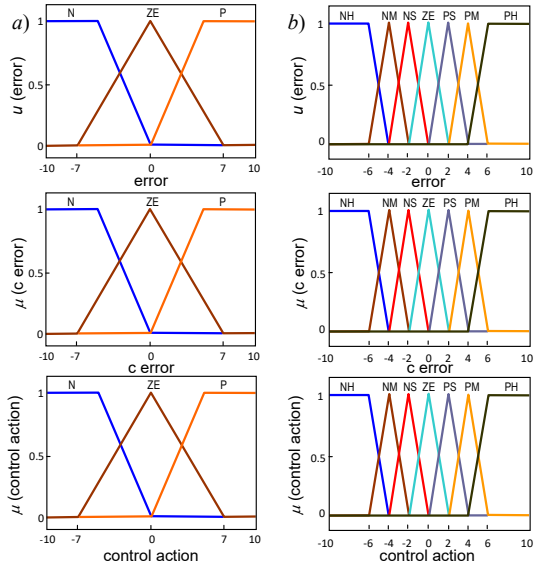

Fig. 6. Membership functions of input/output variables: *a*) current; *b*) speed

The fuzzy inference system uses a 49-rule decision matrix (Table 3) to determine the controller's output response based on the inputs E and ΔE. Each rule is expressed in standard If–Then format and governs the control action accordingly.

Table 3

The rule base for controlling the speed

ΔE \ E	NH	NM	NS	ZE	PS	PM	PH
NH	NH	NH	NH	NH	NM	NS	ZE
NM	NH	NH	NH	NM	NS	ZE	PS
NS	NH	NH	NM	NS	ZE	PS	PM
ZE	NH	NM	NS	ZE	PS	PM	PH
PS	NM	NS	ZE	PS	PM	PH	PH
PM	NS	ZE	PS	PM	PH	PH	PH
PH	ZE	PS	PM	PH	PH	PH	PH

Some of the rules in Table 3 can be interpreted as follows: for example, if the speed error E is PM and its derivation ΔE is also PM, then the torque increment ΔT_{em} should be PH. In this case, both the error and its rate of change indicate a moderate increase in speed, and a fast corrective action is required – hence, a high positive torque increment is needed.

The same methodology used to design the speed controller is applied to develop the current controller, with appropriate adaptations to account for the different control objectives. The current controller includes the following features.

The input error E: instead of being equal to $E = \Omega^* - \Omega$, it will be equal with $E = i_{ds}^* - i_{ds}$ for the 1st fuzzy controller of current i_{ds} and $E = i_{qs}^* - i_{qs}$ for the 2nd fuzzy controller of current i_{qs}.

The fuzzy controller outputs are V_{ds} for the i_{ds} current controller and V_{qs} for the i_{qs} current controller.

The inner current control loop operates with faster dynamics than the outer speed loop, maintaining the required cascade control hierarchy.

As shown in Fig. 6,*b*, both input variables (the error E and its derivative ΔE) are triangular membership functions, which are divided into 3 fuzzy subsets: Positive (P), Negative (N), and Zero (ZE). This control strategy uses a compact 9-rule inference system (Table 4) to determine the appropriate output response for all possible combinations of input conditions. This minimalist fuzzy partitioning ensures high computational efficiency while maintaining accurate and robust current regulation.

Table 4

The rule case for controlling the currents

ΔE \ E	N	ZE	P
N	N	N	ZE
ZE	N	ZE	P
P	ZE	P	P

Discussion of simulation. Using MATLAB/Simulink, simulations were conducted to evaluate the vector speed control of the 2 series-connected machines in the multi-machine system. The simulation results demonstrate the dynamic responses of the multi-machine system under various operating conditions. To verify that both machines can be controlled independently despite their series connection, a sequence of simulation tests was performed. The speed, current, and torque responses of the 2 unloaded machines are presented in Fig. 7, 8.

In the 1st test, machine 1 was commanded to change speed from +150 rad/s to –150 rad/s at t = 0.5 s, while machine 2 was initially set to run at +200 rad/s, then reversed to –200 rad/s at the same instant (t = 0.5 s).

Both machines were subjected to load torques equal to 100 % of the rated torque corresponding to their reference speeds, applied in the interval t = [0.15–0.3] s. Additionally, load steps were applied at t = 0.2 s for machine 1 and at t = 0.4 s for machine 2.

Figure 8 presents the simulation results for the 2nd test scenario, in which the reference speeds are reversed: machine 1 switches from +200 rad/s to –200 rad/s, and machine 2 – from –200 rad/s to +200 rad/s. These reversals are initiated at t = 0.7 s. Additionally, load torques are applied to both machines during the interval t = [0.2–0.4] s.

From Fig. 7, 8 it is evident that decoupled control is successfully maintained. The independent operation of each machine remains unaffected by the other, with no observable interference or degradation in performance.

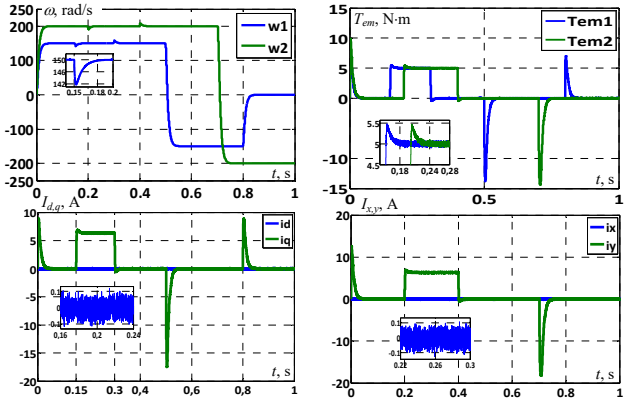

Fig. 7. The PMSM system's dynamic behavior under a 5 N·m load applied during intervals [0.15–3] s and [0.2–0.4] s with subsequent step changes in speed reference

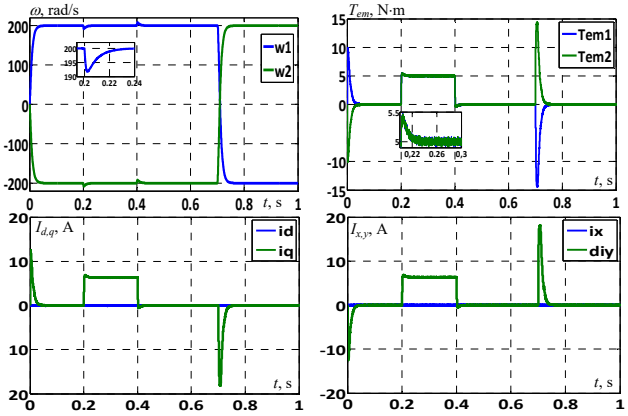

Fig. 8. The dynamic behavior of the PMSM under a 5 N·m load applied during the interval [0.2–0.4] s followed by step variations in speed reference for both machines

Test of robustness. To evaluate the impact of parameter variations on control performance, a robustness test was conducted (Fig. 9). In this test, the motors operate at their nominal reference speeds, while the inertia parameters J_1 and J_2 of both machines are doubled to assess the controllers resilience under mechanical changes. Figure 9 shows the resulting speed and torque responses. The results clearly indicate that parameter variations have a more significant effect on the performance of the classical PI controller compared to the FLC. The FLC demonstrates superior robustness, maintaining stable speed tracking and torque control despite the increased inertia. These findings confirm that the proposed fuzzy controllers are more tolerant of system variations and offer enhanced reliability.

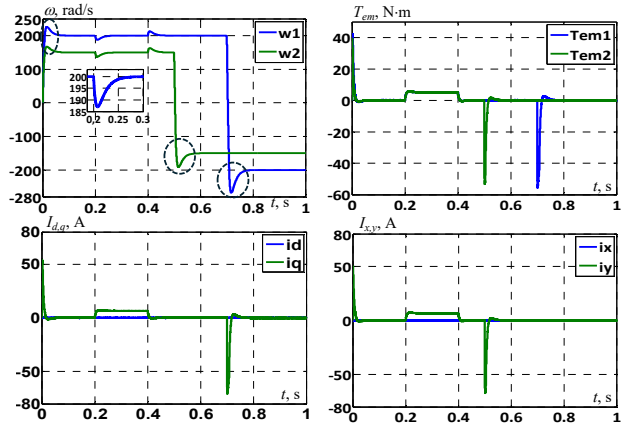

a

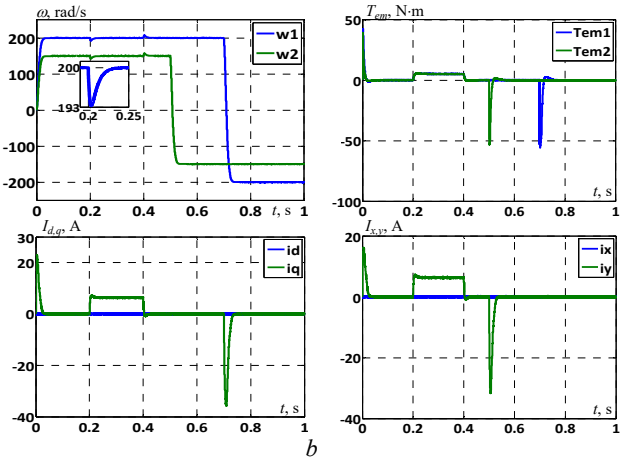

b

Fig. 9. PMSM's responses at J_k variations for both machines: *a* – with PI controllers; *b* – with FLC controllers

Conclusions. This paper presents a dual 5-phase drive system powered by a 12-switch asymmetrical 19-level inverter and controlled using fuzzy logic. The proposed approach enables independent vector control of 2 series-connected machines with reduced hardware complexity.

Simulation results show that the fuzzy controller significantly outperforms the conventional PI controller, achieving a settling time of 0.06 s compared to 0.15 s, a speed error of 0.4 % versus 1.9 %, and a 47 % torque ripple reduction. It also maintains stability under doubled inertia, where PI fails. The inverter achieves THD below 4.5 % and reduces the switch count by 66 %, confirming the system's efficiency, robustness, and suitability for compact, high-performance applications.

Conflict of interest. The authors declare that they have no conflicts of interest.

REFERENCES

1. Park H., Kim T., Suh Y. Fault-Tolerant Control Methods for Reduced Torque Ripple of Multiphase BLDC Motor Drive System Under Open-Circuit Faults. *IEEE Transactions on Industry Applications*, 2022, vol. 58, no. 6, pp. 7275-7285. doi: https://doi.org/10.1109/TIA.2022.3191633.

2. Bhuvaneswari G., Nagaraju. Multi-Level Inverters – A Comparative Study. *IETE Journal of Research*, 2005, vol. 51, no. 2, pp. 141-153. doi: https://doi.org/10.1080/03772063.2005.11416389.

3. Nageswar Rao B., Suresh Y., Aditya K., Naik B.S., Karunakaran E. Design and implementation of novel multilevel inverter with full DC-utilization. *International Journal of Electronics*, 2025, vol. 112, no. 6, pp. 1212-1231. doi: https://doi.org/10.1080/00207217.2024.2370904.

4. Gopinath B., Suresh S., Jayabaskaran G., Geetha M. Renewable energy resource integrated multilevel inverter using evolutionary algorithms. *Automatika*, 2024, vol. 65, no. 3, pp. 1061-1078. doi: https://doi.org/10.1080/00051144.2024.2329494.

5. Sagvand F., Siahbalaee J., Koochaki A. An Asymmetrical 19-Level Inverter with a Reduced Number of Switches and Capacitors. *Electronics*, 2023, vol. 12, no. 2, art. no. 338. doi: https://doi.org/10.3390/electronics12020338.

6. EL Magri A., Lajouad R., Kissaoui M., Chakir M., Bouattane O., Chakir F. Design and analysis of a new multi-level inverter topology with a reduced number of switches and controlled by PDPWM technique. *International Journal of Electrical and Computer Engineering Systems*, 2023, vol. 14, no. 5, pp. 593-600. doi: https://doi.org/10.32985/ijeces.14.5.11.

7. Kakar S., Ayob S.B.M., Iqbal A., Nordin N.M., Arif M.S.B., Gore S. New Asymmetrical Modular Multilevel Inverter Topology With Reduced Number of Switches. *IEEE Access*,

2021, no. 9, pp. 27627-27637. doi: https://doi.org/10.1109/ACCESS.2021.3057554.
8. Djafer L., Taleb R., Mehedi F. Dspace implementation of real-time selective harmonics elimination technique using modified carrier on three phase inverter. *Electrical Engineering & Electromechanics*, 2024, no. 5, pp. 28-33. doi: https://doi.org/10.20998/2074-272X.2024.5.04.
9. Ebrahimi F., Wndarko N.A., Gunawan A.I. Wild horse optimization algorithm implementation in 7-level packed U-cell multilevel inverter to mitigate total harmonic distortion. *Electrical Engineering & Electromechanics*, 2024, no. 5, pp. 34-40. doi: https://doi.org/10.20998/2074-272X.2024.5.05.
10. Nouaoui T., Dendouga A., Bendaikha A. Speed control of PMSM using a fuzzy logic controller with deformed MFS tuned by a novel hybrid meta-heuristic algorithm. *Electrical Engineering*, 2024, vol. 106, no. 6, pp. 6927-6939. doi: https://doi.org/10.1007/s00202-024-02404-w.
11. Thakre K., Mohanty K.B., Kommukuri V.S., Chatterjee A., Nigam P., Gupta S.K. Modified cascaded multilevel inverter for renewable energy systems with less number of unidirectional switches. *Energy Reports*, 2022, no. 8, pp. 5296-5304. doi: https://doi.org/10.1016/j.egyr.2022.03.167.
12. Antar R.K., Hussein T.A., Abdullah A.M. Design and implementation of reduced number of switches for new multilevel inverter topology without zero-level state. *International Journal of Power Electronics and Drive Systems (IJPEDS)*, 2022, vol. 13, no. 1, pp. 401-410. doi: https://doi.org/10.11591/ijpeds.v13.i1.pp401-410.
13. Fnaiech M.A., Betin F., Capolino G.-A., Fnaiech F. Fuzzy Logic and Sliding-Mode Controls Applied to Six-Phase Induction Machine With Open Phases. *IEEE Transactions on Industrial Electronics*, 2010, vol. 57, no. 1, pp. 354-364. doi: https://doi.org/10.1109/TIE.2009.2034285.
14. Hadjidj N., Benbrahim M., Ounnas D., Mouss L.H. Global maximum power point tracking method for photovoltaic systems using Takagi-Sugeno fuzzy models and ANFIS approach. *Electrical Engineering & Electromechanics*, 2025, no. 2, pp. 31-38. doi: https://doi.org/10.20998/2074-272X.2025.2.05.
15. Ali A.R., Antar R.K., Abdulghafoor A.G.A. Harmonics mitigation technique for asymmetrical multilevel inverter fed by photovoltaic sources. *Bulletin of Electrical Engineering and Informatics*, 2024, vol. 13, no. 2, pp. 865-873. doi: https://doi.org/10.11591/eei.v13i2.6607.
16. Li Z., Jiang D., Sun W. Zero Common-Mode Voltage Overmodulation Strategy for Flying Capacitor Three-Level Inverter With Capacitor Voltage Control. *IEEE Journal of Emerging and Selected Topics in Power Electronics*, 2025, vol. 13, no. 5, pp. 6575-6587. doi: https://doi.org/10.1109/JESTPE.2025.3589774.
17. Memon M.A., Siddique M.D., Mekhilef S., Mubin M. Asynchronous Particle Swarm Optimization-Genetic Algorithm (APSO-GA) Based Selective Harmonic Elimination in a Cascaded H-Bridge Multilevel Inverter. *IEEE Transactions on Industrial Electronics*, 2022, vol. 69, no. 2, pp. 1477-1487. doi: https://doi.org/10.1109/TIE.2021.3060645.
18. Sadoughi M., Pourdadashnia A., Farhadi-Kangarlu M., Galvani S. PSO-Optimized SHE-PWM Technique in a Cascaded H-Bridge Multilevel Inverter for Variable Output Voltage Applications. *IEEE Transactions on Power Electronics*, 2022, vol. 37, no. 7, pp. 8065-8075. doi: https://doi.org/10.1109/TPEL.2022.3146825.
19. Jahan H.K., Abapour M., Zare K., Hosseini S.H., Blaabjerg F., Yang Y. A Multilevel Inverter With Minimized Components Featuring Self-Balancing and Boosting Capabilities for PV Applications. *IEEE Journal of Emerging and Selected Topics in Power Electronics*, 2023, vol. 11, no. 1, pp. 1169-1178. doi: https://doi.org/10.1109/JESTPE.2019.2922415.
20. Foti S., Scimone T., Oteri A., Scelba G., Testa A. A Reduced Switch Count, Self-Balanced, 13-Level Inverter Based on a Dual T-Type Configuration. *IEEE Transactions on Power Electronics*, 2023, vol. 38, no. 9, pp. 11010-11022. doi: https://doi.org/10.1109/TPEL.2023.3281679.
21. Benkahla M., Taleb R., Boudjema Z. A new robust control using adaptive fuzzy sliding mode control for a DFIG supplied by a 19-level inverter with less number of switches. *Electrical Engineering & Electromechanics*, 2018, no. 4, pp. 11-19. doi: https://doi.org/10.20998/2074-272X.2018.4.02.
22. Rodriguez J., Franquelo L.G., Kouro S., Leon J.I., Portillo R.C., Prats M.A.M., Perez M.A. Multilevel Converters: An Enabling Technology for High-Power Applications. *Proceedings of the IEEE*, 2009, vol. 97, no. 11, pp. 1786-1817. doi: https://doi.org/10.1109/JPROC.2009.2030235.
23. Song-Manguelle J., Mariethoz S., Veenstra M., Rufer A. A generalized design principle of a uniform step asymmetrical multilevel converter for high power conversion. *European Conference on Power Electronics and Applications (EPE'01)*, 2001, Graz, Austria.
24. Srinivasan G.K., Rivera M., Loganathan V., Ravikumar D., Mohan B. Trends and Challenges in Multi-Level Inverter with Reduced Switches. *Electronics*, 2021, vol. 10, no. 4, art. no. 368. doi: https://doi.org/10.3390/electronics10040368.
25. Bessaad T., Taleb R., Chabni F., Iqbal A. Fuzzy adaptive control of a multimachine system with single inverter supply. *International Transactions on Electrical Energy Systems*, 2019, vol. 29, no. 10, art. no. e12070. doi: https://doi.org/10.1002/2050-7038.12070.
26. Ayada A., Guiza D., Ounnas D., Tidjani N. Design and control of a DC-DC buck converter using discrete Takagi-Sugeno fuzzy models. *Electrical Engineering & Electromechanics*, 2025, no. 3, pp. 53-58. doi: https://doi.org/10.20998/2074-272X.2025.3.08.

Received 20.05.2025
Accepted 06.07.2025
Published 02.11.2025

T. Bessaad [1], *Associate Professor,*
A. Benbouali[1], *Associate Professor,*
K. Khelifi Otmane[2], *Associate Professor,*
R. Taleb[1], *Professor,*
H. Sahraoui[1], *Associate Professor,*
A. Iqbal [3], *Professor,*
[1] Electrical Engineering Department, Faculty of Technology, Laboratoire Génie Electrique et Energies Renouvelables (LGEER), Hassiba Benbouali University, Chlef, Algeria,
e-mail: t.bessaad@univ-chlef.dz (Corresponding Author).
[2] Automatic and Electrotechnical Department, Saad Dahlab University – Blida 1, Blida, Algeria,
[3] Electrical Engineering Department, Qatar University, Doha, Qatar.

How to cite this article:
Bessaad T., Benbouali A., Khelifi Otmane K., Taleb R., Sahraoui H., Iqbal A. Inverter fuzzy speed control of multi-machine system series-connected fed by a single five-phase an asymmetrical 19-level inverter with less number of switches. *Electrical Engineering & Electromechanics*, 2025, no. 6, pp. 8-14. doi: https://doi.org/10.20998/2074-272X.2025.6.02